

Supporting Information

Acceptor-donor-acceptor-type Molecules with large electrostatic potential difference for Effective NIR Photothermal Therapy

Kexin Fan¹, Ludan Zhang², Qinqiu Zhong², Yanhe Xiang¹, Bowei Xu*¹, Yuguang Wang*²

¹ State Key Laboratory of Chemical Resource Engineering, College of Materials Science and Engineering

Beijing University of Chemical Technology

Beijing 100029, China

E-mail: xubowei@buct.edu.cn

² National Engineering Laboratory for Digital and Material Technology of Stomatology Center of Digital Dentistry

Peking University School and Hospital of Stomatology

Beijing 100081, China

E-mail: wangyuguang@bjmu.edu.cn

Structural Characterizations of Materials

Y6: $^1\text{H NMR}$ (400 MHz, Chloroform- d) δ 9.15 (s, 2H), 8.56 (dd, $J = 10.0, 6.5$ Hz, 2H), 7.71 (t, $J = 7.5$ Hz, 2H), 4.88 – 4.66 (m, 4H), 3.23 (s, 4H), 2.15 – 2.04 (m, 2H), 1.93 – 1.81 (m, 4H), 1.61 – 0.93 (m, 55H), 0.88 – 0.64 (m, 18H).

BTP-eC9: $^1\text{H NMR}$ (400 MHz, Chloroform- d) δ 9.18 (s, 2H), 8.80 (s, 2H), 7.96 (s, 2H), 4.85 – 4.66 (m, 4H), 3.24 (t, $J = 7.9$ Hz, 4H), 2.17 – 2.07 (m, 2H), 1.93 – 1.83 (m, 4H), 1.28 (s, 56H), 0.88 (s, 18H), 0.73 – 0.59 (m, 13H).

GPC for PY-DT: $M_n = 9.86$ kDa, $M_w = 14.8$ kDa, PDI = 1.509.

GPC for PZT- γ : $M_n = 11.3$ kDa, $M_w = 23.2$ kDa, PDI = 2.050.

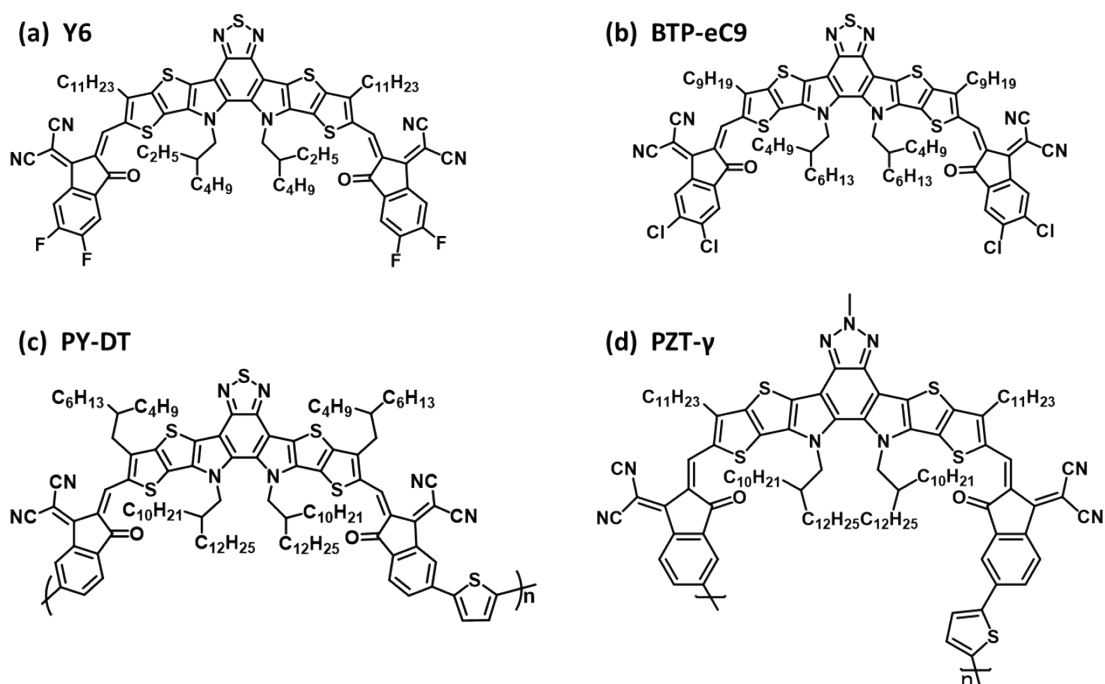


Figure S1. Chemical structure of four photosensitizers (a) Y6, (b) BTP-eC9, (c) PY-DT and (d) PZT- γ used in this Work

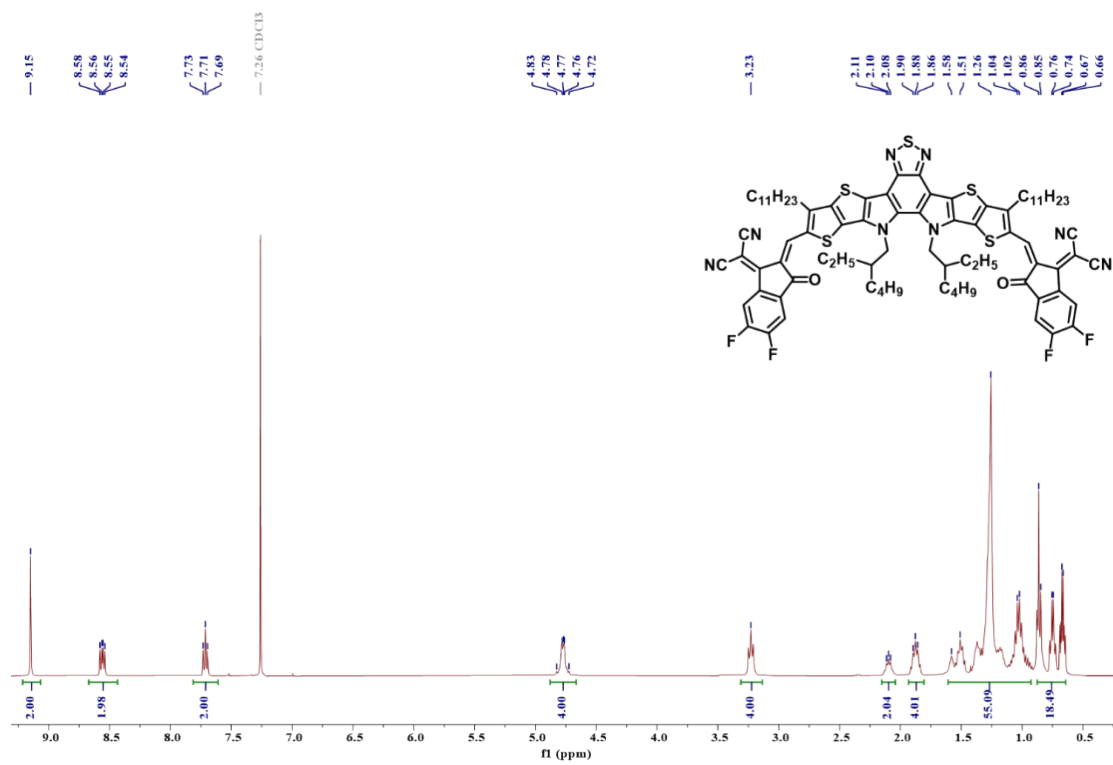


Figure S2. ¹H NMR (400 MHz, CDCl₃) spectrum of Y6

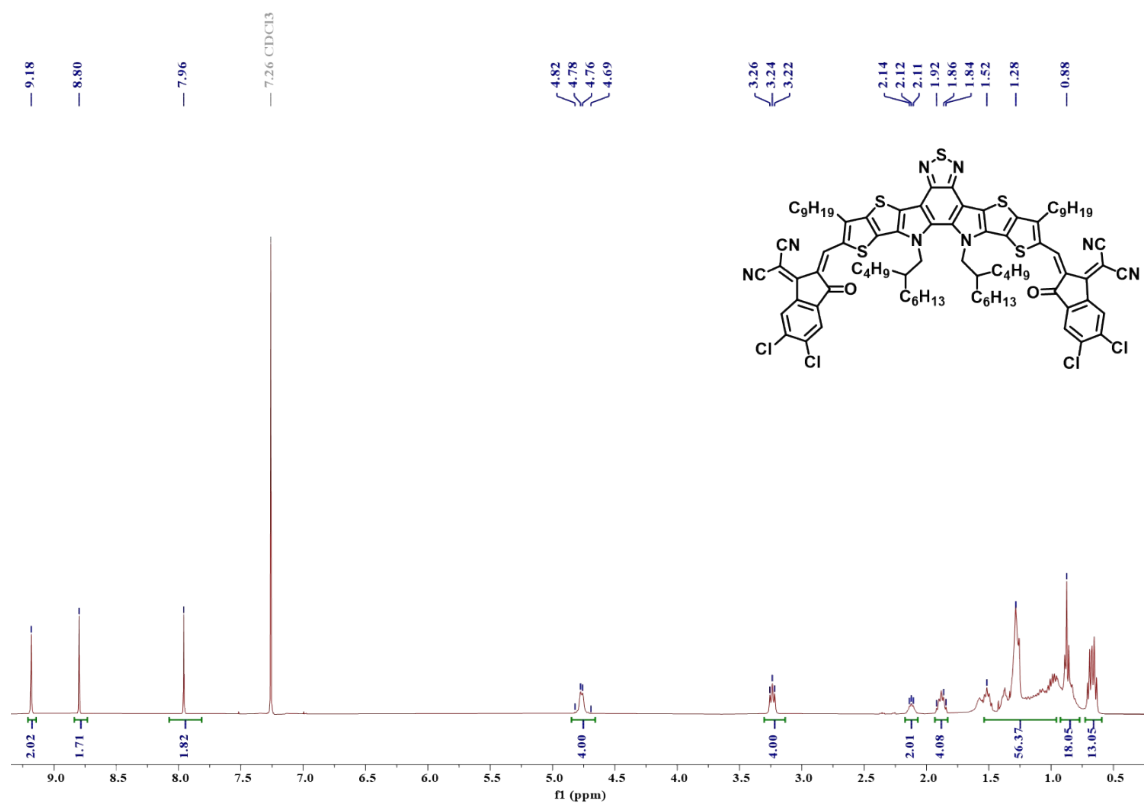


Figure S3. ¹H NMR (400 MHz, CDCl₃) spectrum of BTP-eC9

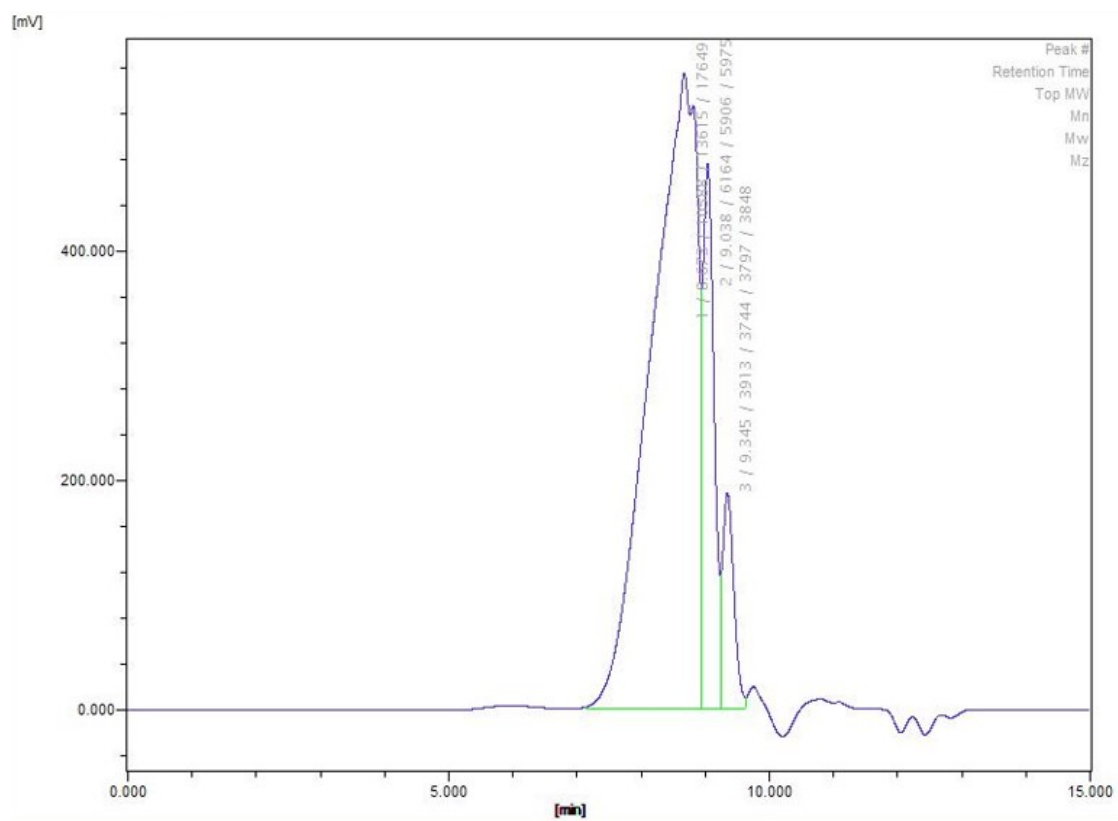


Figure S4. Gel-permeation chromatography data diagram for PY-DT

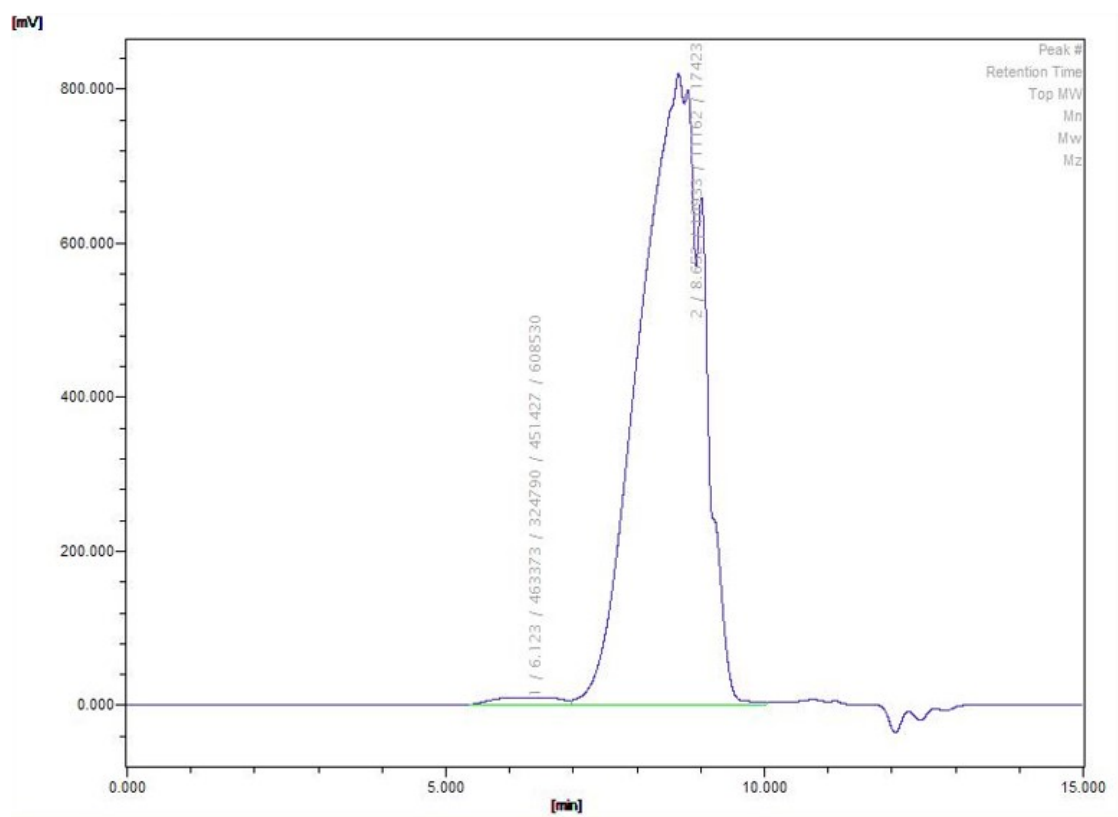


Figure S5. Gel-permeation chromatography data diagram for PZT- γ

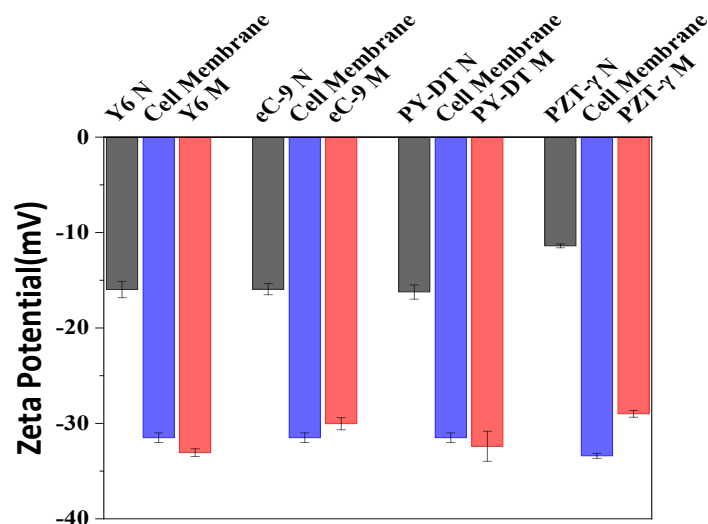


Figure S6. Zeta potential changes of bare NPs, Erythrocyte membrane, and Erythrocyte membrane coated NPs, respectively.

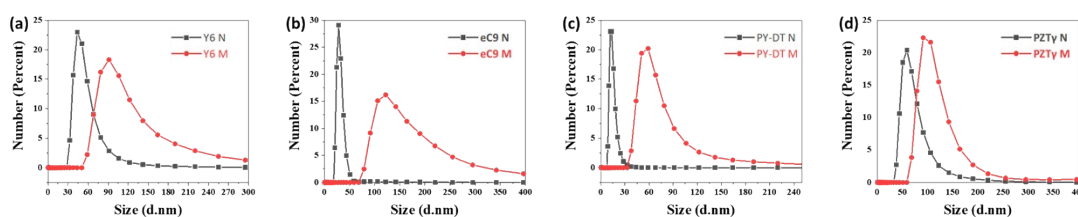


Figure S7. Size changes of (a) Y6, (b) BTP-eC9, (c) PY-DT and (d) PZT- γ NPs before and after coating with Erythrocyte membrane.

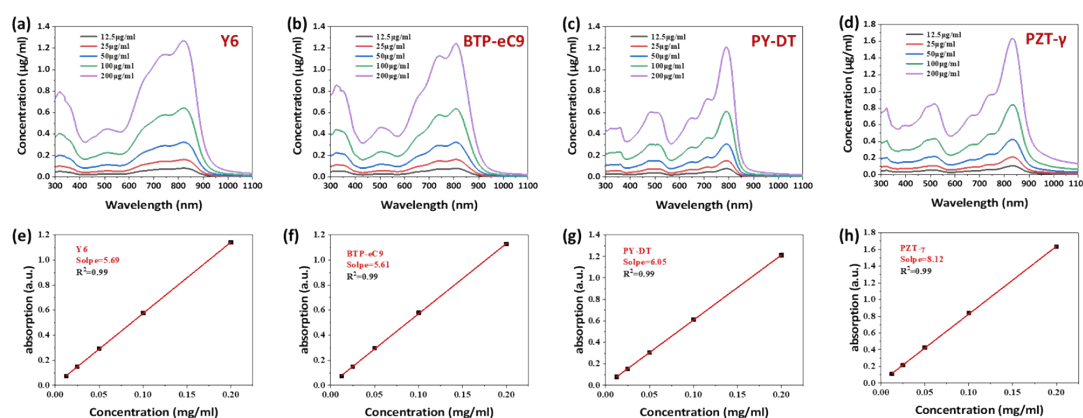


Figure S8. Measurement of the mass extinction coefficient of NPs in water. UV-vis-NIR spectra with (a) Y6, (b) BTP-eC9, (c) PY-DT and (d) PZT- γ NPs in water at different concentrations .Absorbance of NPs at 808 nm plotted as a function of the concentration of NPs in water. The slopes represent the mass extinction coefficients of (e) Y6, (f) BTP-eC9, (g) PY-DT and (h) PZT- γ NPs at

808 nm in water. The slope represents the mass extinction coefficient of PQIA-BDTP NPs at 808 nm in water.

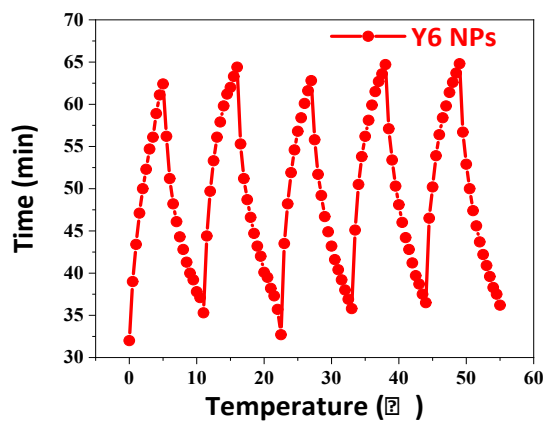


Figure S9. Temperature profiles of Y6 NPs aqueous solution for five ON/OFF cycles.

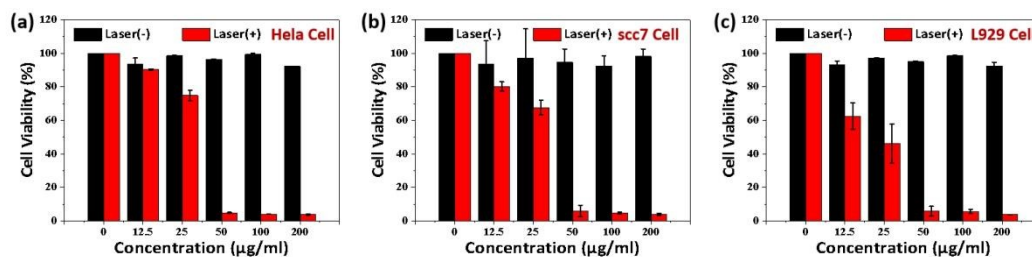


Figure S10. In vitro cytotoxicity of the Y6 NPs. Viability of (a) HeLa, (b) scc7, (c) L929 cells incubated at varying concentrations with or without 808 nm laser irradiation for 10 min ($1 \text{ W} \cdot \text{cm}^{-2}$).